

Multiwavelength Diffraction and Apodization Using Binary Superimposed Gratings

Ivan A. Avrutsky, Martin Fay, *Student Member, IEEE*, and J. M. Xu, *Senior Member, IEEE*

Abstract—The binary superimposed grating (BSG), consisting of equal-size segments of two possible values of refractive index and capable of effecting multiwavelength reflection, offers ease of fabrication and great versatility in guided-wave wavelength-division-multiplexing (WDM) applications. We present an analytical formula for the coupling strength of a BSG as a function of segment size, and verify it with numerical transfer matrix simulations of the grating reflectance spectra. Perfect agreement is found for a single grating, and values $\sim 10\%$ – 12% less than predicted for 2–11 superimposed gratings. Subdividing the grating into sections of grouped segments permits step-like apodization, while maintaining binary index and base segment size. Sidemode suppression ratios (SMSR's) of 27 and 16 dB are computed for single-peak and 11-peak BSG's respectively.

Index Terms—Apodization, diffraction gratings, distributed Bragg reflector (DBR) lasers, laser resonators, wavelength-division multiplexing (WDM).

I. INTRODUCTION

THE RAPID development of wavelength-division-multiplexing (WDM) systems has produced great demand for compact selective multiwavelength tuning elements. Where high efficiency and selectivity are desired, an attractive choice is the Bragg grating, which can be superimposed to produce compact multiwavelength devices [1]. In semiconductors, however, reproduction of an arbitrary index profile is impeded by the high nonlinearity of exposure and etching processes. Single-depth etching greatly simplifies processing; the resulting gratings are then “binary” in that etch depth, and consequently effective index, take on one of two values. It is therefore of great interest to develop a binary structure which emulates multiwavelength diffraction: the binary superimposed grating (BSG).

A binary grating consists of segments of equal size and of two possible values of modal index. The simplest example is a rectangular profile grating with 50% duty cycle, where segment size s is half the grating period Λ . An open question is: what grating strength can be achieved when s is not an integer fraction of the half-period? This problem becomes especially important in the case of superimposed gratings of closely spaced periods Λ_j ($j = 1, \dots, N$), when having integer ratios between s and all Λ_j is impossible.

In some cases, it is desirable to have a grating whose coupling coefficient κ is not constant, but instead varies along

its length. This is known as “apodization,” and for bell-like profiles of coupling strength can yield strong suppression of sidelobes occurring in the vicinity of the Bragg wavelength.

For etched grating structures, a number of apodization schemes have been presented. Varying etch depth is perhaps the most obvious approach, as in principle it allows continuous variation of grating strength. Talneau *et al.* have used multiple holographic exposures of photoresist to produce multiwavelength gratings with variable etch-depth [2] and single-wavelength gratings with a Moiré variation in duty cycle [3]. Duty cycle can be varied more easily with sampled gratings, which consist of alternate grating and unetched sections [4], [5]. While simple, this approach yields a variation in effective index, necessitating careful phase-matching between grating sections if superior sidemode suppression ratios (SMSR's) are desired. Another approach consists of a double layer of buried gratings [6], for which the upper grating may be selectively etched to locally set κ to one of two values. For this approach, however, variation in κ is limited by the number of grating layers. Finally, one can imagine varying the bar/space ratio of individual grating teeth, as suggested in [7] and as has been done for holographic gratings [8]; this, however, requires precise control during both the writing and etching stages, and can also produce undesired resonance from its bell-like profile of average modal index [9].

For ease of fabrication, an attractive solution would be one which maintains uniform etch depth, segment size, and duty cycle, avoiding reproducibility problems, easing pattern resolution tolerances, and preventing chirp-induced resonance respectively. We show here that both apodization and multiwavelength characteristics can be implemented easily and effectively within the confines of the BSG approach.

II. COUPLING STRENGTH OF A BINARY GRATING

Let us consider a binary grating of length $L = Ms$, where M is the number of segments. Its longitudinal modal index profile, $n(x)$, can be represented as a sum of Π -type “teeth,” as illustrated in Fig. 1:

$$n(x) = n + \frac{\Delta n}{2} \sum_{i=1}^M v_i \Pi_s(x, s(i-1/2)) \quad (1)$$

where average index n and contrast Δn are wavelength- and mode-dependent, v_i is $+1$ or -1 , and $\Pi_s(x, x_i)$ is defined as

$$\Pi_s(x, x_i) = \begin{cases} 1, & |x - x_i| < s/2 \\ 0, & |x - x_i| > s/2 \end{cases} \quad (2)$$

Manuscript received December 4, 1997; revised February 5, 1998. This work was supported by Nortel and by the NSERC.

The authors are with the Department of Electrical and Computer Engineering, University of Toronto, Toronto, ON, M5S 3G4 Canada.

Publisher Item Identifier S 1041-1135(98)03791-4.

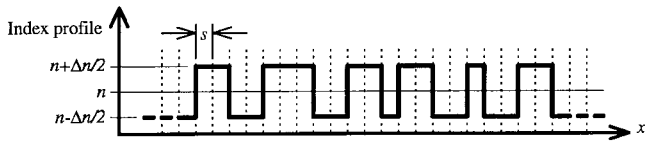


Fig. 1. Schematic diagram of the index profile of a binary superimposed grating, showing segment size s and index contrast Δn .

The coupling strength κ_s for a waveguide mode with wavelength $\lambda_B = 2n\Lambda$ is proportional to the Fourier harmonic of $n(x)$ at the spatial frequency $2\pi/\Lambda$. For the profile defined by (1) and (2), Fourier integration along the grating length (using $\sin(2\pi x/\Lambda)$ with no loss of generality) yields

$$\kappa_s = \frac{\Delta n}{nL} \sin\left(\frac{\pi s}{\Lambda}\right) \sum_{i=1}^M v_i \sin\left(\frac{2\pi}{\Lambda} s(i-1/2)\right). \quad (3)$$

If we want to maximize κ_s for a single-wavelength grating (i.e., single values of λ_B and Λ), we need to maximize the sum in (3), which immediately yields the simple rule

$$v_i = \text{sgn}(f(s(s-1/2))) \quad (4)$$

$$f(x) = \sin\left(\frac{2\pi}{\Lambda} x\right). \quad (5)$$

To estimate the sum in (3), we shift all points $x_i = s(i-1/2)$ by an integer number of periods Λ such that $x_i \in [0, \Lambda]$, and assume that they are distributed randomly and uniformly. This assumption is violated when s is a rational fraction of Λ :

$$s = \frac{P}{Q}\Lambda \quad (6)$$

where P and Q are integers with no common factors. However, beyond relation (6) and supposing $M = L/s$ is large (M is typically a few thousand), we can replace the sum defined in (3) and (4) by an integration over the period Λ and get

$$\kappa_s = \frac{\Delta n}{n\Lambda} \frac{|\sin(\pi s/\Lambda)|}{\pi s/\Lambda} = \kappa_0 \frac{|\sin(\pi s/\Lambda)|}{\pi s/\Lambda} \quad (7)$$

where $\kappa_0 = \Delta n/n\Lambda$ is the coupling strength for a ‘‘conventional’’ rectangular grating with 50% duty cycle. Thus, for single-wavelength implementations, $\kappa_s < \kappa_0$, and (7) shows the price of adopting a binary scheme.

We now return to the case of relation (6). From (3), followed by a simple albeit tedious trigonometric manipulation, we obtain the following, where we have assumed that $L \gg P\Lambda$:

$$\kappa_{PQ} = \frac{\Delta n}{n\Lambda} \frac{|\sin(\pi P/Q)|}{P \sin(\pi/Q)} \times \begin{cases} 1, & \text{if } Q \text{ is even} \\ \cos(\pi/2Q), & \text{if } Q \text{ is odd} \end{cases} \quad (8)$$

For $P = 1$ and Q even, (8) yields the coupling coefficient for a rectangular grating with 50% duty cycle: $\kappa|_{P=1, Q=2q} = \kappa_0$. For any $P > 1$ and $Q \rightarrow \infty$, the coupling coefficient defined by (8) asymptotically approaches that defined by (7). In fact, the case of (6) has little practical importance, because the peculiarities of $\kappa(s)$ near s satisfying (6) are very narrow [10]. Moreover, for the case of emulating N superimposed gratings, it is unlikely that (6) would be met for several periods Λ_j . In any event, BSG design algorithms can be used to optimize the

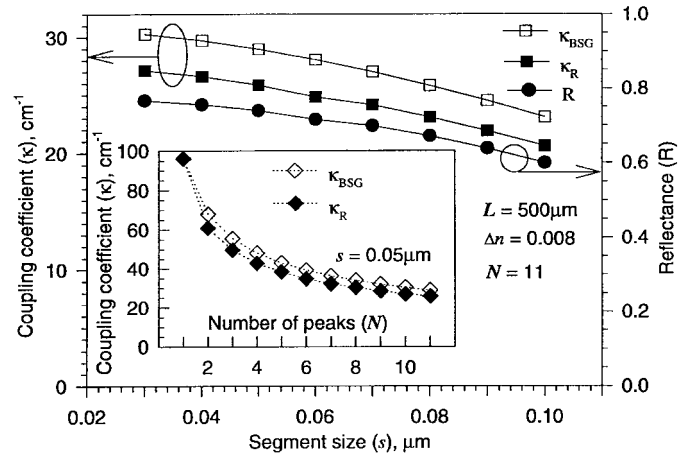


Fig. 2. Comparison of $\kappa(s)$ for an 11-peak BSG, as predicted by (10) and obtained using (11) from computed reflectance spectrum. *Inset*: comparison of $\kappa(s = 50 \text{ nm})$ as given by (10) and (11), as a function of number of peaks N .

relative weights of the constituent pitches Λ_j to selectively adjust reflectance peaks.

It is not so evident how to optimally design a BSG for $N > 1$ —a variety of approaches are possible. One method follows from the above-mentioned algorithm for $N = 1$, by replacing (5) with a superposition of sinusoids

$$f(x) = \sum_{j=1}^N a_j \sin\left(\frac{2\pi}{\Lambda_j} x + \psi_j\right) \quad (9)$$

where the amplitudes a_j and phases ψ_j are free parameters that can be used to optimize the BSG’s performance. For example, we have found that relative amplitudes must be adjusted to produce a comb-like grating reflectance spectrum with equal peak reflectance at all Bragg wavelengths.

To determine the coupling strength for a number $N > 1$ of superimposed gratings, one can use an approach based on Parseval’s theorem, as suggested in [11] for the case of superstructure gratings, which (assuming small variations in $|\sin(\pi s/\Lambda_j)|/(\pi s/\Lambda_j)|$) introduces a factor of $1/\sqrt{N}$

$$\kappa_{\text{BSG}} = \frac{1}{\sqrt{N}} \frac{\Delta n}{n\Lambda} \frac{|\sin(\pi s/\Lambda)|}{\pi s/\Lambda}. \quad (10)$$

To verify (7), (8), and (10), we designed BSG structures using (1), (2), (4), and (9); computed their reflectance spectra by a transfer matrix method; and determined the coupling coefficient from peak reflectance R

$$\kappa_R = \frac{1}{2L} \ln\left(\frac{1+\sqrt{R}}{1-\sqrt{R}}\right) \quad (11)$$

which follows from the well-known reflectance formula for a lossless Bragg grating: $R = \tanh^2(\kappa L)$. Fig. 2 shows a comparison of coupling coefficients calculated analytically using (10), and numerically using (11) with computed reflectance values. Perfect agreement is observed for $N = 1$, while for $N = 2 - 11$ the numerically calculated coupling strength is 10%–12% less than that determined analytically. This good agreement establishes the usefulness of (10) in predicting BSG coupling strength for any N .

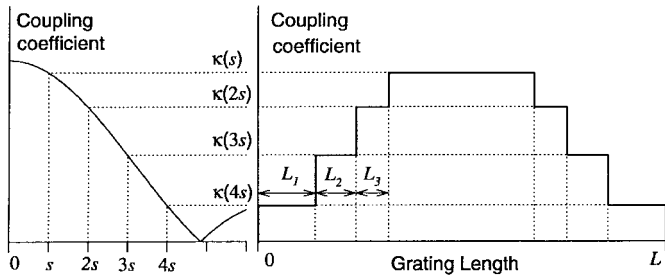


Fig. 3. Piecewise continuous apodization scheme, yielding four values of κ while maintaining constant segment size, etch depth, and average effective index.

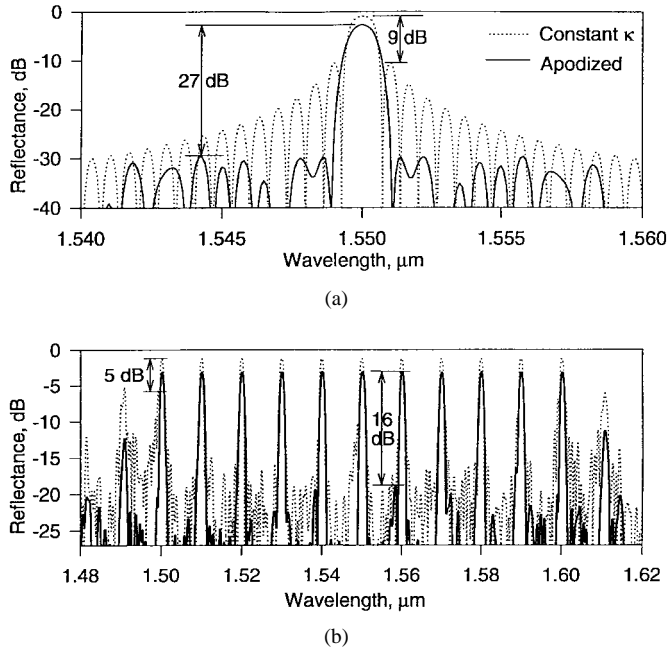


Fig. 4. Reflectance spectra for constant- κ and apodized grating structures of length $L = 500 \mu\text{m}$ and segment size $s = 50 \text{ nm}$ with (a) 1 peak, $\Delta n = 0.0024$ and (b) 11 peaks, $\Delta n = 0.008$.

III. APODIZATION SCHEME

The above $\kappa(s)$ dependence suggests an elegant way of implementing apodization while maintaining all the advantages of the binary approach. If segment size is a few times less than the grating period, we can divide the grating into subsections, each a binary grating with segment size $s, 2s, \dots, ms$ ($ms < \Lambda$), thus varying coupling strength; the overall structure is still a binary grating with segment size s , subjected to group binarization of neighboring segments. This allows apodization to be effected in piecewise constant form, as illustrated in Fig. 3. The subsection lengths can be optimized to maximize the SMSR.

Fig. 4 shows a comparison of reflectance spectra for BSG's with and without four-level apodization, for $L = 500 \mu\text{m}$ and $s = 50 \text{ nm}$. The minimum feature size, strictly bounded by s and generally a multiple thereof, is in this case 100 nm , well within the capabilities of electron beam lithography. For a single grating ($N = 1$), apodization yields 27-dB SMSR, in comparison to only 9 dB for a structure with equal L and Δn but uniform strength. Moreover, using the same subsection

lengths—that is, without additional optimization—we found that for a BSG with $N = 11$ [Fig. 3(b)], apodization improved SMSR from $\sim 5 \text{ dB}$ (worst-case sidemode) to about 16 dB.

Apodization does come at the price of decreased reflectance and slightly increased peak width; for most applications, however, this is more than compensated by the dramatic improvement in SMSR. This effect results from a reduced abruptness of changes in distributed reflectance along the grating, which in effect suppresses the high-frequency components of the grating zone. For binary etching schemes, this must be accomplished without recourse to varying Δn , which leads to low-tolerance designs such as those discussed in the introduction. Varying duty cycle suffers from the drawback that minimum κ is constrained by minimum feature size, and is also very susceptible to exposure and etching errors. The BSG implementation suggested here is the first solution which makes use of uniform etch depth, segment size, and duty cycle, and promises great ease of manufacture.

IV. CONCLUSION

The coupling strength of binary superimposed gratings is derived analytically, and confirmed numerically using a transfer matrix method. An apodization scheme for BSG's is suggested, which utilizes the dependence of coupling strength on segment size. The scheme retains the benefits of the binary approach, and is completely compatible with existing one-step etched-grating techniques.

REFERENCES

- [1] V. Minier, A. Kévkian, and J.M. Xu, "Diffraction characteristics of superimposed gratings in planar waveguides," *IEEE Photon. Technol. Lett.*, vol. 4, pp. 1115–1118, 1992.
- [2] A. Talneau, C. Ougier, and S. Slemptes, "Multiwavelength grating reflectors for widely tunable laser," *IEEE Photon. Technol. Lett.*, vol. 8, pp. 497–499, 1996.
- [3] A. Talneau, J. Charil, A. Ougazzaden, and J. C. Bouley, "High power operation of phase-shifted DFB lasers with amplitude modulated coupling coefficient," *Electron. Lett.*, vol. 28, pp. 1395–1396, 1992.
- [4] Y. Shibata, T. Tamamura, S. Oku, and Y. Kondo, "Coupling coefficient modulation of waveguide grating using sampled grating," *IEEE Photon. Technol. Lett.*, vol. 6, pp. 1222–1224, 1994.
- [5] S. Hansmann, H. Hillmer, H. Walter, H. Burkhard, B. Hübner, and E. Kuphal, "Variation of coupling coefficients by sampled gratings in complex coupled distributed-feedback lasers," *IEEE J. Select. Topics Quantum Electron.*, vol. 1, pp. 341–345, 1995.
- [6] S. Nilsson, T. Kjellberg, T. Klinga, J. Wallin, K. Streubel, and R. Schatz, "DFB laser with nonuniform coupling coefficient realized by double-layer buried grating," *IEEE Photon. Technol. Lett.*, vol. 5, pp. 1128–1131, 1993.
- [7] B. E. Little and C. Wu, "Window functions for ideal response in distributed feedback reflection filters," *IEEE Photon. Technol. Lett.*, vol. 9, pp. 76–78, 1997.
- [8] C. Robledo-Sánchez, G. Camacho-Basilio, A. Jaramillo-Núñez, and A. Cornejo-Rodríguez, "Binary grating with a variable bar/space ratio following a geometrical progression," *Opt. Commun.*, vol. 119, pp. 465–470, 1995.
- [9] T. A. Strasser *et al.*, "UV-induced fiber grating OADM devices for efficient bandwidth utilization," in *OFC '96*, San Jose, CA, 1996, pt. A, pp. 360–363, postdeadline paper PD8.
- [10] I. A. Avrutsky, D. S. Ellis, A. Tager, H. Anis, and J. M. Xu, "Design of widely tunable semiconductor lasers and the concept of binary superimposed gratings (BSG)," *IEEE J. Quantum Electron.*, vol. 34, pp. 729–741, Apr. 1998.
- [11] H. Ishii, H. Tanobe, F. Kano, Y. Tohmori, Y. Kondo, Y. Yoshikuni, "Quasicontinuous wavelength tuning in super-structure-grating (SSG) DBR lasers," *IEEE J. Quantum Electron.*, vol. 32, pp. 433–441, 1996.